BIOCHEMISTRY
including biophysical chemistry & molecular biology

Article

pubs.acs.org/biochemistry

Micelle-Catalyzed Domain Swapping in the GlpG Rhomboid Protease Cytoplasmic Domain

Houman Ghasriani,[†] Jason K. C. Kwok,[†] Allison R. Sherratt,[‡] Alexander C. Y. Foo,[†] Tabussom Qureshi,[†] and Natalie K. Goto*[,†,‡]

[†]Department of Chemistry and [‡]Department of Biochemistry, Microbiology and Immunology, University of Ottawa, Ottawa, Ontario, Canada K1N 6N5

Supporting Information

ABSTRACT: Three-dimensional domain swapping is a mode of self-interaction that can give rise to altered functional states and has been identified as the trigger event in some protein deposition diseases, yet rates of interconversion between oligomeric states are usually slow, with the requirement for transient disruption of an extensive network of interactions giving rise to a large kinetic barrier. Here we demonstrate that the cytoplasmic domain of the *Escherichia coli* GlpG rhomboid protease undergoes slow dimerization via domain swapping and that micromolar concentrations of micelles can be used to enhance monomer−dimer exchange rates by more than 1000-fold. Detergents bearing a phosphocholine headgroup are shown to be true catalysts, with hexadecylphosphocholine reducing the 26 kcal/mol free energy barrier by >11 kcal/mol while preserving the 5 kcal/mol difference between monomer and dimer states. Catalysis involves the formation of a micelle-bound intermediate with a partially unfolded structure that is primed for domain swapping. Taken together, these results are the first to demonstrate true catalysis for domain swapping, by using micelles that work in a chaperonin-like fashion to unfold a kinetically trapped state and allow access to the domain-swapped form.

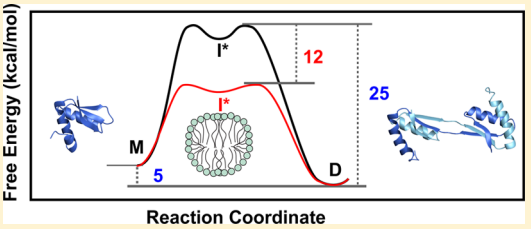

Three-dimensional domain swapping is a mechanism for oligomerization whereby a structural element from one subunit exchanges with the equivalent element in another subunit, engaging in the same interactions that are found in the monomeric state.[1] Exchanged elements typically come from the N- or C-terminus and can be formed by a compact globular domain or by secondary structure elements that are an integral component of each domain structure.[2,3] Although domain swapping is a relatively unusual mode of interaction, with only ∼60 structures of domain-swapped proteins available,[4] a wide range of structures undergo this type of interaction, leading to suggestions that domain swapping can be induced in almost any protein fold.[3]

Domain swapping can provide a mechanism for the regulation of functional states, in some cases giving rise to altered ligand binding (e.g., heparin binding by a PWWP domain[5]) or changes in enzyme activity (e.g., RNase A allostery[6]). These interactions have also attracted an increasing amount of attention for potential contributions to protein deposition diseases,[7,8] with crystal structures of domain-swapped species captured for disease-associated proteins such as cystatin C,[9] β2-microglobulin,[10] and α1-antitrypsin[11] that appear to be intermediates in the fibril formation pathway.[12−14] Similarly, the human prion protein responsible for the spongiform encephalopathy Creutzfield-Jakob disease has been crystallized as a disulfide bond-linked domain-swapped dimer[15] that has formed the basis for a model of fibril formation via runaway domain swapping.[16]

A number of pioneering studies have identified factors that influence domain swapping propensities, including hinge−loop sequence,[17,18] length,[19,20] and strain,[19,21,22] as well as the role of protein unfolding in some domain swapping mechanisms (e.g., p13suc1[23,24] and the first domain of cell adhesion protein CD2[20]). Nonetheless, the study of domain swapping under physiological conditions can be complicated by the presence of a large kinetic barrier separating monomeric and domain-swapped states, because a significant number of interactions must be disrupted to allow exchange between monomeric and domain-swapped species. While the formation of a domain-swapped state can be facilitated by exposure of high concentrations of protein to a denaturing environment, these are not conditions that are typically encountered in physiological systems. In addition, the use of chemical denaturants can alter the equilibrium (e.g., stefin[25] or Fis1[26]) or even promote the formation of different types of domain-swapped states that differ from the biologically relevant species.[27] These issues highlight the difficulties that exist in the identification of factors that can influence domain swapping rates and energetics and how these might pertain to the formation of domain-swapped species *in vivo*.

Here we have found that the cytoplasmic domain from the *Escherichia coli* GlpG rhomboid protease can undergo domain

Received: July 25, 2014
Revised: August 26, 2014
Published: August 27, 2014

swapping dimerization that is slow under physiologically relevant conditions but can be accelerated by exposure to micelles. We establish that zwitterionic micelles play a catalytic role in the exchange reaction, with a positive correlation between micelle size and rate enhancement. The structural properties of the micelle-bound intermediate suggest that this process involves the formation of a partially unfolded state. Overall, these results are the first to demonstrate a catalytic role for micelles in domain swapping and raise the possibility that lipid−protein interactions could in some cases facilitate the formation of domain-swapped species.

MATERIALS AND METHODS

Kinetics. C-Terminally hexahistidine-tagged CytD (residues 1−61 of *E. coli* GlpG) was expressed and purified as previously described.[28] Monomeric and dimeric species were isolated in the final size exclusion chromatography step on a Superdex-75 10/300 GL column (GE Healthcare) in 25 mM phosphate buffer (pH 6.5), 150 mM NaCl, and 100 μM EDTA and stored at 4 °C. To measure the rate of dimerization, 0.25 mM samples of monomeric CytD were incubated at elevated temperatures (45−60 °C) to stimulate exchange. Aliquots of each sample were removed after a range of incubation times and rapidly cooled on ice. Size exclusion chromatography was then performed at room temperature for each sample on the Superdex-75 column, and peak volumes of the monomeric and dimeric species in each elution profile were used to calculate the relative population of the monomeric and dimeric state at each time point. Both dimer formation and dimer dissociation were found to follow classical first-order chemical kinetics for a two-state system undergoing reversible exchange:

$$\mathrm{M} + \mathrm{M} \underset{k_{-1}}{\overset{k_1}{\rightleftharpoons}} \mathrm{D} \tag{1}$$

where M is the monomeric CytD and D is the dimeric form.[29] Most reactions were conducted starting with the purely monomeric state as the reactant species. Under these conditions, the integrated rate equation for the loss of monomer in the reversible dimerization reaction is given by

$$f^{\mathrm{M}} = f_{\mathrm{eq}}^{\mathrm{M}} + (f_{\mathrm{o}}^{\mathrm{M}} - f_{\mathrm{eq}}^{\mathrm{M}})\mathrm{e}^{-k_{\mathrm{ex}}t} \tag{2}$$

where f^{M} is the fraction of monomeric CytD at time t, $f_{\mathrm{eq}}^{\mathrm{M}}$ is the monomer fraction at equilibrium, $f_{\mathrm{o}}^{\mathrm{M}}$ is the initial fraction of monomeric CytD, and k_{ex} is the rate of exchange between monomeric and dimeric states given by

$$k_{\mathrm{ex}} = 2k_1 + k_{-1} \tag{3}$$

Nonlinear least-squares fitting was conducted to determine the value of k_{ex} for each rate profile. Because at equilibrium

$$k_1 f_{\mathrm{eq}}^{\mathrm{M}} = \frac{1}{2} k_{-1} f_{\mathrm{eq}}^{\mathrm{D}} \tag{4}$$

The fraction of monomeric CytD at equilibrium could be used with eq 2 to find k_1 and k_{-1}. Equilibrium populations were also used to determine the dimer dissociation constant:

$$K_{\mathrm{d}} = \frac{[\mathrm{M}]_{\mathrm{eq}}^{\ 2}}{[\mathrm{D}]_{\mathrm{eq}}} = \frac{2(f_{\mathrm{eq}}^{\mathrm{M}})^2}{f_{\mathrm{eq}}^{\mathrm{D}}}[\mathrm{CytD}] \tag{5}$$

where $[\mathrm{M}]_{\mathrm{eq}}$ and $[\mathrm{D}]_{\mathrm{eq}}$ represent the concentrations of the monomer and dimer at equilibrium, respectively, and $[\mathrm{CytD}]$ is the total concentration of CytD used. The effect of detergents or denaturants on the rate of dimer formation was also investigated using this same method, with all experiments performed at 45 °C to allow direct comparison to rate constants determined in the absence of additives at this temperature. Dodecyl maltoside (DDM) and decyl-, dodecyl-, tridecyl-, and hexadecylphosphocholines (Fos10, Fos12, Fos13, and Fos16, respectively) were purchased from Affymetrix, and 1-palmitoyl-2-hydroxy-*sn*-glycero-3-phospho(1′-*rac*-glycerol) (LPPG) was purchased from Avanti Polar Lipids. Second-order rate constants (k_2) for detergent-catalyzed reactions were determined by measurement of k_{ex} over a range of detergent concentrations. A linear relationship between k_{ex} and micelle concentration was found in all cases, and the slope of this line was taken as k_2. Rate constants were also measured in the absence of detergents or in the presence of Fos16 over a range of temperatures and used in the Eyring equation to determine the free energy of activation:

$$\ln\left(\frac{k}{T}\right) = -\frac{\Delta^{\ddagger}H^{\circ}}{RT} + \frac{\Delta^{\ddagger}S^{\circ}}{R} + \frac{k_{\mathrm{B}}}{h} \tag{6}$$

Nuclear Magnetic Resonance (NMR) Spectroscopy and CytD Dimer Structure Calculation. NMR samples contained 0.7−1.0 mM uniformly labeled ^{15}N-labeled or ^{13}C- and ^{15}N-labeled CytD in 25 mM phosphate buffer (pH 6.5), 150 mM NaCl, and 0.1 mM EDTA. All NMR spectra were recorded at 25 °C, on a Varian Inova 500 (University of Ottawa NMR Facility), Bruker AVANCE III 600 MHz (Centre for Vaccine Evaluation, Health Canada), or Varian Inova 800 (Quebec/Eastern Canada High Field NMR Facility) spectrometer, the latter two being equipped with a triple-resonance cryogenic probe. Chemical shifts of the dimeric state were assigned using ^{15}N HSQC, ^{13}C HSQC, HNCACB, CBCA(CO)NH, HCCH-COSY, and ^{15}N NOESY-HSQC spectra, which was facilitated by comparison with shifts from the monomeric state. Data were processed by NMRPipe[30] and analyzed with NMRView.[31] Average backbone amide chemical shift differences ($\Delta\delta$) between monomeric and dimeric forms were calculated according to the formula

$$\Delta\delta = \sqrt{(\Delta\delta_{\mathrm{H^N}})^2 + (\Delta\delta_{\mathrm{N}}/5)^2} \tag{7}$$

where $\Delta\delta_{\mathrm{H^N}}$ and $\Delta\delta_{\mathrm{N}}$ are the chemical shift differences between monomeric and dimeric species for the amide proton and nitrogen atoms, respectively.

To identify the intermolecular interface, a heterodimeric protein sample was prepared by mixing equimolar amounts of monomeric ^{13}C- and ^{15}N-labeled CytD with monomeric unlabeled CytD, which was then incubated with 2.5 mM Fos16 at room temperature for 1 h to promote dimer formation. Size exclusion chromatography was performed to isolate the dimeric state, which was then used to record an F1-^{13}C,^{15}N-filtered/F3-^{13}C-edited NOESY spectrum (τ_{mix} = 90 ms). Manual assignment of 131 intermolecular upper-bound distance restraints from this spectrum was provided as input, along with ϕ and ψ dihedral angles derived from TALOS,[32] to guide automatic NOE assignment of three-dimensional (3D) ^{15}N-edited NOESY HSQC (τ_{mix} = 75 ms) and 3D aliphatic ^{13}C-edited NOESY-HSQC (τ_{mix} = 90 ms) spectra in the torsion angle dynamics program CYANA version 2.1.[33] Hydrogen bond restraints were also included for residues in secondary structure elements that showed protection from amide proton solvent exchange, as determined by the persistence of the corresponding peaks in the ^{1}H−^{15}N HSQC spectrum acquired

dx.doi.org/10.1021/bi500919v | *Biochemistry* 2014, 53, 5907−5915

after buffer exchange into D_2O. The ensemble represents the 20 lowest-energy structures of the 200 generated in the final round of CYANA.

Circular Dichroism Spectroscopy. CD spectra were recorded on a Jasco J-815 circular dichroism spectropolarimeter with a 0.1 cm path length quartz cell at 45 °C. Spectra reflect an average of eight scans recorded from 250 to 200 nm with a 0.5 nm step resolution, a speed of 20 nm/min, and a bandwidth of 1.0 nm. Samples typically contained ~5 μM monomeric CytD in 25 mM phosphate buffer (pH 6.5) and 150 mM sodium chloride, in the presence or absence of 20 mM Fos16. At this concentration, ~99% of the sample is monomeric at equilibrium.

The secondary structure content of CytD in the presence and absence of Fos16 was estimated using CDPro[34,35] in conjunction with JASCO's spectral analysis software. Average structure percentages were calculated using the SP43 reference protein set with SELCON3, CONTIN, and CDSSTR.[35] Outputs from the three programs were averaged to determine the percent helix, sheet, and random/undefined contributions to secondary structure.

Equilibrium Binding Measurement. CD was used to monitor the interaction between CytD and Fos16, because there was an increase in the intensities at 207 and 222 nm upon micelle binding. CytD (5 μM) in 25 mM phosphate buffer (pH 6.5) and 150 mM NaCl was incubated with Fos16 detergents at a range of concentrations. To minimize the impact of small variations in CytD concentration from sample to sample, the amount of CytD bound to Fos16 was measured by taking the ratio (r) of the ellipticity at 222 nm, a wavelength that showed a large change upon micelle binding (Θ_{222}), to that of a wavelength that showed almost no change (e.g., 217 nm, Θ_{217}). The fraction of CytD bound to Fos16 micelles (f_b) was calculated using the equation

$$f_b = \frac{r - r_o}{r_{max} - r_o} \tag{8}$$

where $r = (\Theta_{222}/\Theta_{217})$, r_o is the initial ratio of ellipticities (in the absence of micelles), and r_∞ is the ratio when all CytD is micelle-bound. The fraction bound was plotted as a function of Fos16 micelle concentration ([micelle]), calculated using the equation

$$[\text{micelle}] = \frac{[\text{Fos16}] - \text{cmc}}{N} \tag{9}$$

with a critical micelle concentration (cmc) and aggregation number (N) of 13 μM and 178, respectively, as reported by the manufacturer (Anatrace). Nonlinear least-squares fitting to the equation

$$f_b = \Big[[\text{CytD}] + [\text{micelle}] + K_d - \sqrt{([\text{CytD}] + [\text{micelle}] + K_d)^2 - 4[\text{CytD}][\text{micelle}]}\Big] / \Big(2[\text{CytD}]\Big) \tag{10}$$

was used to find the dissociation constant for the micelle−CytD interaction, because the detection limits of the CD experiment necessitated the use of CytD concentrations that were similar in magnitude to the K_d of the micelle−CytD interaction.[36]

RESULTS

The GlpG Cytoplasmic Domain Forms a Domain-Swapped Dimer in Solution. During the course of our previous work on the structured portion of the cytoplasmic domain (CytD) from the *E. coli* GlpG rhomboid (residues 1−61),[28] size exclusion chromatography profiles in the final purification step showed the presence of a dimeric state. This dimer was stable at room temperature, with conversion into an equilibrium mixture of a monomer and dimers occurring only upon exposure to elevated temperatures [e.g., 45 °C (Figure 1A)]. Purely monomeric CytD also underwent conversion to a dimeric state upon being subjected to these conditions (Figure 1B). Using integrated peak volumes from chromatography profiles, monomer and dimer populations were monitored as a function of time. For both the forward (i.e., dimer formation) and reverse (dimer dissociation) reactions, decay profiles could be fit to the first-order integrated rate equation for a reversible two-state system to obtain the rate constant for exchange (k_{ex}) as shown in Figure 1C. Equilibrium populations could be used with k_{ex} to obtain the rate constant for forward (k_1) and reverse reactions (k_{-1}) over a range of temperatures, allowing Eryring parameters for the activation barrier to be determined (Figure 1C, inset). A significant activation enthalpy was found to separate the two states, with a $\Delta^{\ddagger}H$ of 74 ± 1 kcal mol^{-1} (85 ± 2 kcal mol^{-1}) for the forward (reverse) reaction (Table 1), with a half-life for the monomer of 1.9 days at 45 °C. Thermal denaturation of the monomer as monitored by CD confirmed that CytD was folded over the range of temperatures used in this analysis, with a melting temperature of ~90 °C (Figure S1 of the Supporting Information).

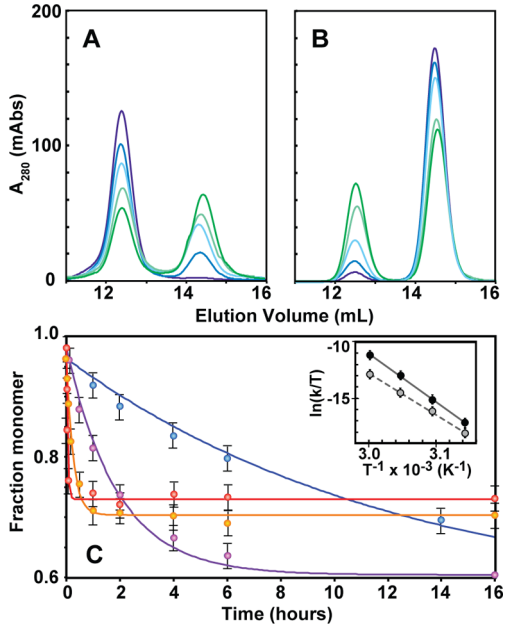

Figure 1. Kinetics of CytD monomer−dimer interconversion. Size exclusion chromatography profiles of 250 μM CytD in the predominantly (A) dimeric or (B) monomeric state before (purple) and after incubation at 45 °C for 1 h (dark blue), 4 h (light blue), 9 h (A) or 14 h (B) (light green) and 26 h (dark green). (C) Time dependence for the monomer-to-dimer transition at 45 °C (blue), 50 °C (purple), 55 °C (orange), and 60 °C (red) and the corresponding Eyring plot (inset) for the monomer-to-dimer (white points) and dimer-to-monomer (black) transition.

dx.doi.org/10.1021/bi500919v | *Biochemistry* 2014, 53, 5907−5915

Table 1. Activation Energy Parameters from Eyring Analysis

	no detergent		with Fos16	
	2M → D	D → 2M	2M → D	D → 2M
$\Delta^{\ddagger}H°$ (kcal/mol)	73.2 ± 0.9	85.0 ± 1.7	20.1 ± 1.5	26.1 ± 0.4
$\Delta^{\ddagger}S°$ (cal K^{-1} mol^{-1})	147.1 ± 2.8	185.7 ± 5.3	16.4 ± 5.0	37.3 ± 1.2
$\Delta^{\ddagger}G°$ at 45 °C (kcal/mol)	26.5 ± 1.3	25.9 ± 2.4	14.9 ± 2.2	14.2 ± 0.5

Two-dimensional $^{1}H-^{15}N$ correlation HSQC spectra acquired for the monomer and dimer showed a subset of peaks with significant shift differences between the two states, localizing to the turn region connecting β2 and β3 in the monomer structure (Figure S2 of the Supporting Information). Differences calculated between experimentally determined backbone chemical shifts and random coil values[37,38] showed differences between monomer and dimer species for only residues in this turn (shown for $^{13}C\alpha$ shifts in Figure S2C of the Supporting Information), indicating that the structure of the dimer resembles that of the monomer. These observations, along with the large activation energy for interconversion, provided strong evidence that dimerization was occurring via a 3D domain swap. This was confirmed by intermolecular NOEs (Figure S3 of the Supporting Information) used to determine the solution NMR structure of the dimer (Figure 2). This elongated structure has two globular domains that resemble the monomeric state of the protein, with the C-terminal α-helix (α2) and central β-strand (β3) being swapped between protomers (Figure 2). Significant changes in backbone dihedral angles between monomeric and dimeric states were observed for His32 and Asn33 (Figure S4 of the Supporting Information), as is required to convert the turn between β2 and β3 into the extended conformation seen in the dimer.

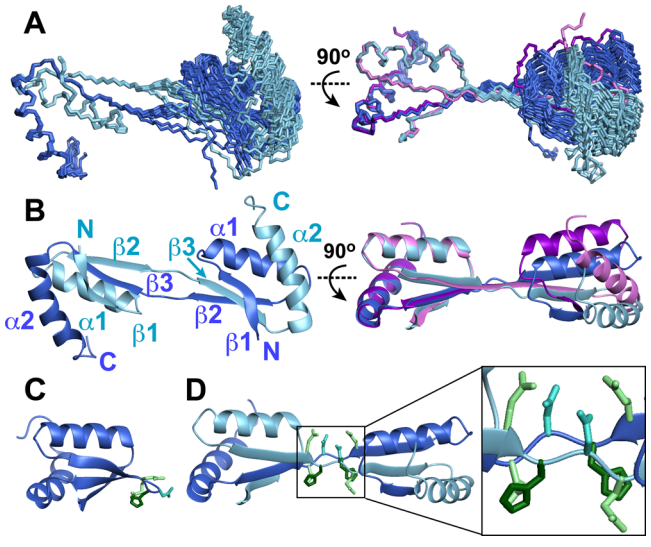

Figure 2. Solution NMR structure of the CytD dimer. (A) Two views of the 20 lowest-energy structures of the CytD dimer produced in CYANA 2.1, with residues 1−30 from chain A (light blue) and residues 35−60 from chain B (dark blue) superimposed [Protein Data Bank (PDB) entry 2MJA, BMRB entry 19713]. The relative arrangement of protomers with respect to each other is poorly defined relative to that of a single protomer. Superposition with the X-ray structure (PDB entry 4HDD) colored purple is shown at the right. (B) Ribbon diagram representation of the lowest-energy conformer with secondary structure elements labeled in the same color that is used for each chain. (C) Lowest-energy conformer of the CytD monomer (PDB entry 2LEP), in the same orientation as shown for the left-hand protomer of the dimer on right-hand side of panel B. (D) Same view as panel B (right-hand side) with side chains from residues in the hinge region highlighted in the expanded view. His32 is colored dark green and Asn33 turquoise, and Gln31 and Gln34 are colored light green (these side chains are also shown for the monomer in the same color scheme in panel C). All structural figures were made in MOLMOL.[65]

Given the extended structure of the hinge region, few NOE restraints are available to define it, thereby limiting the global precision of the ensemble (Table S1 of the Supporting Information). Intermolecular NOEs were nonetheless observed in these hinge residues (Figure S3 of the Supporting Information), suggesting a propensity for intermolecular interactions between the two strands. This is supported by heteronuclear $\{^{1}H\}-^{15}N$ NOEs measured over the hinge region, which were similar in magnitude to those from the structured domains (Figure S5 of the Supporting Information). This could reflect the potential for inter- and intramolecular hydrogen bonding interactions involving a cluster of side chain amides on one face of the hinge formed by Asn33 and Gln31 (Figure 2D). These additional interactions between polypeptide chains in the hinge may be at least partly responsible for the enthalpy change that more than compensates for the loss of entropy associated with dimerization, as was shown in the linear van't Hoff relationship obtained for this interaction (Figure S6 of the Supporting Information). These interactions also appear to increase the stability of the hydrogen bonding network involving the central β3 strand, as backbone amide hydrogen exchange protection factors are higher for the dimer in this region (Figure S7 of the Supporting Information).

At the time that this structure was being refined, a crystal structure of GlpG residues 2−67 was published with its asymmetric unit containing an elongated structure lacking a hydrophobic core.[39] Inspection of symmetry-related molecules showed that this construct formed domain-swapped dimers in the crystal. As shown in Figure 2, the domain-swapped dimer obtained in the crystal is highly similar to the conformation of the dimer in solution. While there do appear to be some differences in the relative orientation of protomers between the solution and crystal structures, these differences are small and may result from crystal packing interactions or the lower precision of the solution structure in hinge residues. Nonetheless, the independent determination of a domain-swapped topology for the CytD dimer in solution confirms that the domain-swapped state captured in the crystal represents the same as we see in solution, and that crystallization is not required for domain swapping to occur.

Catalysis of CytD Domain Swapping. Previous studies of the cytoplasmic domain of the homologous rhomboid from *Pseudomonas aeruginosa* showed interactions with membrane-mimetic detergent micelles.[40,41] To determine whether the *E. coli* homologue possessed similar properties, 2.5 mM hexadecylphosphocholine (Fos16) was added to ^{15}N-labeled monomeric CytD. As shown in the $^{1}H-^{15}N$ HSQC spectrum (Figure 3A), a subset of peaks lost some of their original

dx.doi.org/10.1021/bi500919v | *Biochemistry* 2014, 53, 5907−5915

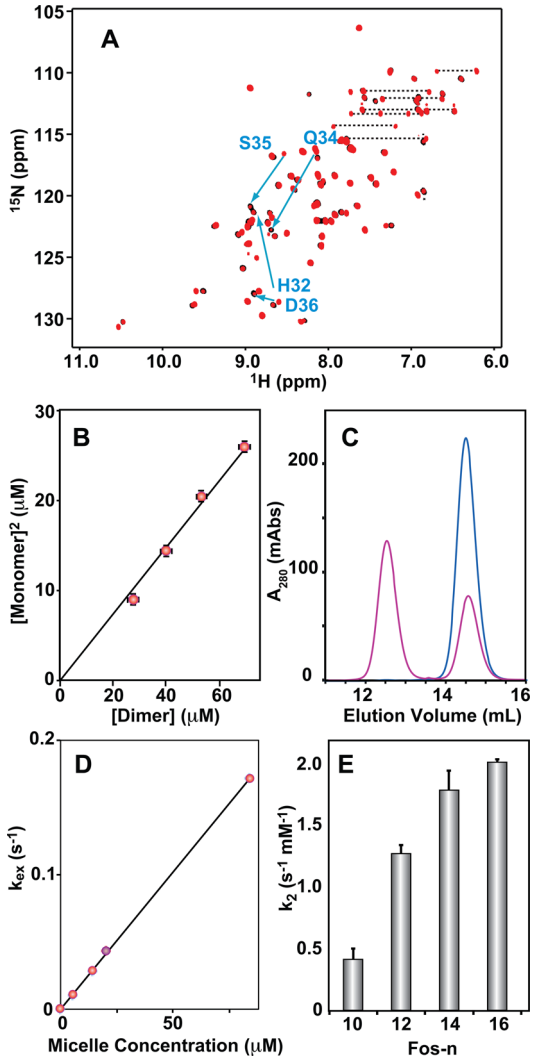

Figure 3. Acceleration of CytD domain swapping by phosphocholine detergents. (A) ^{1}H−^{15}N HSQC spectrum at 25 °C of 0.25 mM monomeric CytD with 2.5 mM Fos16 detergent (red), superimposed on the spectrum of the pure dimer. Diagnostic peaks for monomer and dimer species are connected with arrows. (B) Monomer−dimer equilibrium in the presence of Fos16. The slope of this line gives a dissociation constant of 0.37 mM. (C) Micellar detergent is responsible for the acceleration of domain swapping. Size exclusion chromatography profiles for 0.25 mM CytD after incubation for 1 h at 25 °C with submicellar (2.5 mM, blue) or micellar (15 mM, purple) concentrations of Fos10. (D) CytD dimerization is first-order in Fos16 micelles. Exchange rate constants (k_{ex}) at 45 °C are plotted as a function of micelle concentration. The second-order rate constant obtained from the slope is 2.0 s^{-1} (mM micelles)$^{-1}$. The k_{ex} at 2.5 mM LPPG is colored purple. (E) Second-order rate constants for dimerization in the presence of micelles comprised of Fos*n* where *n* is the number of carbon atoms in the detergent alkyl chain.

intensity, while new peaks appeared at different positions in the spectrum that were identical to those seen for the domain-swapped dimer (Figure S2 of the Supporting Information). Size exclusion chromatography confirmed that the Fos16-treated system was comprised of a mixture of monomeric and dimeric species, even though the temperature of the experiment was too low for interconversion to occur at an appreciable rate in the absence of detergent. Moreover, at 45 °C, the rate constant for interconversion in the presence of 2.5 mM Fos16 was found to be ∼1700-fold faster than the detergent-free reaction (Table 2).

Table 2. Acceleration of CytD Domain Swapping at 45 °C

additive[a]	K_d (mM)	k_{ex} (s^{-1})	*x*-fold acceleration
none	0.36 ± 0.01	(2.0 ± 0.4) × 10^{-5}	1
Fos16	0.35 ± 0.05	0.034 ± 0.010	1700
LPPG	0.68 ± 0.03	0.044 ± 0.016	2200
DDM	0.48 ± 0.13	(12 ± 2) × 10^{-5}	6.0
urea	0.71 ± 0.02	(8.9 ± 1.0) × 10^{-5}	4.5

[a]All detergent concentrations are 2.5 mM, and the urea concentration is 1 M.

This effect was observed over a range of CytD concentrations and gave rise to a linear relationship between the squared concentration of monomer and the dimer concentration, as expected for a monomer−dimer system at equilibrium (Figure 3B). Most strikingly, the equilibrium constant measured in the presence of Fos16 is the same as that measured in the absence of detergent at this temperature (Table 2), demonstrating that Fos16 is acting as a catalyst in the domain swapping reaction.

To determine whether the micelle or the monomeric state of Fos16 was responsible for domain swapping catalysis, we evaluated the activity of a shorter chain phosophocholine detergent that did not form micelles at the concentrations used in the Fos16 experiments. Incubation of a submicellar concentration (2.5 mM) of decylphosphocholine (Fos10) with monomeric CytD did not promote domain-swapped dimer formation at room temperature, while micellar concentrations showed rapid equilibration of the two species (Figure 3C). Further evidence that the micelle is the active species was also provided by the linear relationship observed between pseudo-first-order rate constants measured for dimer formation and Fos16 concentrations (Figure 3D), because increases in the concentration of a detergent above its critical micelle concentration increase the concentration of micelles, but not monomeric detergent. The size of the micelle appears to be important for this effect, with second-order rate constants determined in the presence of phosphocholine detergents of increasing alkyl chain lengths also showing an increase in catalytic activity (Figure 3E).

To identify the characteristics of the micelle that are important for acceleration of domain swapping, rate constants were also measured for dimer formation at 45 °C in the presence of different detergent types (Figure S8 of the Supporting Information and Table 2). While the anionic lysolipid LPPG gave rise to a comparable degree of rate acceleration, the nonionic detergent DDM only weakly promoted exchange. Chemical denaturants were also much less effective at promoting exchange, with 1 M urea being >100-fold less effective than micromolar concentrations of micelles bearing anionic or zwitterionic headgroups (Table 2). Moreover, urea gave rise to a small decrease in the proportion of dimer relative to equilibrium levels obtained in the absence of urea, in contrast with the catalysis by Fos micelles, which did not alter the apparent affinity of CytD dimerization. Overall, these results indicate that the presence of a micellar structure with charges in the headgroup is important for catalysis.

Mechanism of Micelle-Catalyzed Domain Swapping. While the use of micelles to catalyze reactions is well-established in organic chemistry, the mechanism of catalysis for domain swapping is likely to differ from that of synthetic reactions in which selective encapsulation of reactants in the confined volume of the micelle reduces the entropic cost of forming a bimolecular transition state.[42] Instead, we find that

dx.doi.org/10.1021/bi500919v | *Biochemistry* 2014, 53, 5907−5915

dimer formation exhibits first-order kinetics with respect to CytD, indicating that the rate-determining step does not involve the association of two subunits but rather the formation of an intermediate, or excited state, that must be sparsely populated to give rise to the apparent two-state system observed in our experiments. Therefore, the micelle may catalyze the reaction by selective interactions with this intermediate (and its transition state) to lower its energy. This is supported by the reduction in enthalpy required to form the transition state in the presence of Fos16 (Table 1), because favorable interactions between CytD and the micelle could compensate for intramolecular interactions that must be disrupted for domain swapping to occur. Meanwhile, the large increase in entropy that is associated with the formation of the transition state is reduced in the presence of Fos16 (Table 1), as would be expected from the formation of a complex between CytD and the micelle.

To gain structural insight into the nature of the micelle–CytD intermediate, CD spectra were acquired for monomeric CytD in the presence and absence of saturating quantities of Fos16 micelles. As shown in Figure 4A, there is a significant

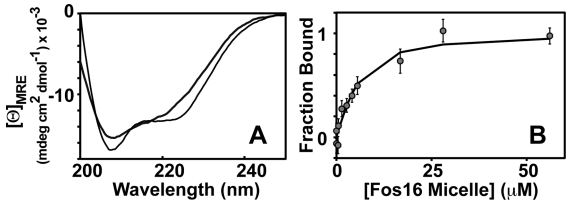

Figure 4. (A) CD spectrum of monomeric CytD in the absence (black) and presence (gray) of 20 mM Fos16 (110 μM micelles) at 45 °C. (B) Equilibrium binding of Fos16 micelles to monomeric CytD at 45 °C, monitored by CD using the ratio of ellipticity at 222 nm to that at 217 nm to give a dissociation constant of 2 ± 1 μM.

change in the shape of the CD spectrum when an excess of Fos16 micelles is added, with an increase in intensity at 207 and 222 nm indicating the transition to α-helical structure. Secondary structure prediction from these spectra confirms this increase in helix content and suggests that it comes at the expense of β and random structure (Table 3). Thermal

Table 3. Percent Secondary Structure Prediction from CD Spectra

	α	β	turn	random
CytD	35 ± 3	17 ± 1	19 ± 1	29 ± 1
CytD with Fos16	45 ± 2	10 ± 1	19 ± 1	26 ± 1

denaturation studies of the micelle-bound state did not show the cooperative loss of structure that would be expected from a folded globular protein (Figure S1 of the Supporting Information), suggesting that the secondary structure elements of the micelle-bound state do not participate in stable tertiary interactions. Overall, these data indicate that the micelle-bound intermediate is not completely unfolded but instead retains significant secondary structure, at least some of which is likely to be non-native.

The change in the shape of the CD spectrum upon binding to Fos16 micelles was used to measure the fraction of CytD bound to micelles at various micelle concentrations. This allowed the dissociation constant of 2 ± 1 μM for this interaction to be measured (Figure 4B), corresponding to a free energy of 8 kcal/mol at 45 °C. This approaches the size of the 11 kcal/mol reduction in the free energy barrier separating monomeric and dimeric states that is provided by Fos16 micelles (Table 1).

DISCUSSION

The study of domain swapping can be complicated by the large kinetic barriers that separate oligomeric states, making it necessary to expose samples to destabilizing conditions that may also alter the free energy difference between these states. However, the use of pH extremes, chemical denaturants, and/or very high concentrations can raise questions regarding the physiological relevance of domain-swapped states that are isolated in this manner. We have found that in the case of GlpG CytD, it is possible to reduce the size of the kinetic barrier without altering the equilibrium between monomeric and domain-swapped dimeric states through transient interactions with Fos16 micelles. The ability of substoichiometric amounts of micelles to significantly accelerate the domain swapping reaction without altering the free energy difference between products and reactants is consistent with the role of the micelle as a catalyst. While detergents have previously been implicated in a small number of cases of domain swapping, a catalytic role for the micelle had not been demonstrated. For example, sodium dodecyl sulfate was shown to promote domain swapping in the pollen allergen, Bet v4;[43] however, this occurred only when submicellar concentrations of detergent were used. Nonionic detergents also induced domain-swapped dimers in the pro-apoptotic Bax protein,[44,45] although it was not shown if the micellar or monomeric state of the detergent was responsible, or if the detergent preserves the free energy difference between monomeric and dimeric states. Therefore, to the best of our knowledge, our results provide the first demonstration that detergent micelles can act as a true catalyst in domain swapping.

Although not previously appreciated, the ability of detergents to catalyze domain swapping is likely to extend to a range of proteins wider than the range that has currently been identified and will be particularly relevant for those involving the formation of a partially unfolded intermediate with some capacity to interact with a detergent micelle. For example, saposin C is capable of forming domain-swapped dimers in solution[46] but can also bind to detergent micelles in a partially unfolded "open" conformation.[47] Cyanovirin-N also undergoes domain-swapped dimer formation by first-order kinetics, with a large degree of unfolding being involved in this process.[48] This must involve a partially or fully unfolded intermediate, likely with exposed hydrophobic residues that could facilitate interactions with a micelle catalyst. The structure and charge characteristics of this intermediate will have some impact on the physical properties of the micelle required to function as a catalyst, with the ideal system being able to interact reversibly with this intermediate. In this respect, the interaction between the Fos16 micelle and CytD appears to be optimal, as micelle binding allows a significant reduction in the energy of the intermediate, but is still transient enough to allow dissociation from the micelle in a state that can allow domain swapping to proceed. Moreover, the micelles can be easily removed by dilution to submicellar concentrations or by size exclusion chromatography in the absence of detergent. Therefore, the study of domain-swapped interactions that involve the formation of a high-energy intermediates could be facilitated

dx.doi.org/10.1021/bi500919v | Biochemistry 2014, 53, 5907–5915

by the use of detergent micelles capable of stabilizing a partially unfolded state.

The ability of the Fos16 micelle to induce a partially unfolded state in CytD bears some similarity to the actions of chaperonins, assisting folding of proteins that form kinetically trapped intermediates along the folding pathway.[49] Chaperonins such as GroEL and GroES can interact with misfolded intermediates in a way that promotes unfolding.[50,51] In the case of CytD, the monomer or dimer could be considered to be a kinetically trapped state, where interactions with the Fos16 micelle can disrupt the fold to produce a partially unfolded state. This differs from previous applications of micelles as chaperones in protein folding reactions, because the role of the micelle in those instances was to bind to an unfolded state produced through exposure to high-temperature conditions or chemical denaturants.[52,53] As seen in chaperones, this interaction prevents aggregation of the hydrophobic segments that become exposed in the unfolded state. However, these micelle−protein complexes were very stable, and therefore, it was necessary to remove the detergent through the addition of detergent-binding agents[52] or enzyme-catalyzed polymerization into a nonmicellar state[53] to allow release of unfolded polypeptides under conditions that promote refolding. In the case of the micelle−CytD interaction, partial unfolding is induced by the interaction with the micelle, producing a state that is capable of undergoing domain swapping association or dissociation, followed by spontaneous release from the micelle to allow the reaction to proceed.

Although the rhomboid has only recently been discovered,[39] accumulating evidence supports a physiological role for the domain-swapped dimer in the GlpG rhomboid from which CytD is derived. In particular, it has been shown that GlpG is dimeric in detergent micelles,[54] and that cleavage of a detergent-solubilized transmembrane substrate by purified GlpG requires conditions that promote the dimeric state.[55] In addition, it appears that CytD domain swapping occurs *in vivo*, because proteolysis of inside-out vesicles made from *E. coli* membranes releases CytD in a stable dimeric state.[55] While it is possible that co- or post-translational factors could facilitate formation of the domain-swapped species,[56] the effect of the micelle on CytD domain swapping may also provide some insight. The integration of full-length GlpG into the lipid membrane may facilitate interactions between CytD and the bilayer surface that creates the activated state required for domain swapping. Local irregularities in bilayer structure such as those suggested in molecular dynamics simulations of GlpG[57−59] could potentially enhance this effect. These deformations could allow increased access to the hydrophobic phase of the membrane, mimicking the dynamic, solvent-accessible nature of the hydrophobic phase of the micelle.

It is interesting to speculate about the effect that local irregularities in lipid structure could have in the nucleation of otherwise rare domain swapping events. This could be of particular relevance for amyloid fibril formation, as it has been suggested that propagated domain swapping is involved in the formation of oligomers on the path to fibril formation.[7,8,10,12,60,61] Fibrils typically accumulate over the course of several years, with *in vitro* studies showing the presence of a lag period that precedes the growth phase.[12,62−64] This lag phase is associated with the time it takes to form a nucleus that can recruit soluble species into the aggregate. Because this nucleus is comprised of domain-swapped oligomers in at least some cases (e.g., cystatin C[12−14]), this raises questions regarding the initiation of fibril formation *in vivo* and whether there are physiologically relevant factors that can promote domain swapping. Conditions that destabilize the soluble species can shorten or eliminate the lag phase *in vitro*, suggesting that exposure to local destabilizing environments could initiate fibril growth *in vivo*. Our demonstration of micelle-catalyzed domain swapping raises the possibility that transient interactions with membranes could trigger one of these nucleating events. Although the soluble state of fibril-forming proteins does not typically have a tendency to bind to lipid membranes, local deformations in lipid structure that increase solvent accessibility of the hydrophobic phase, for example, through the action of curvature-inducing proteins, or by hydrophobic mismatch at the phase boundaries of lipid rafts, could facilitate transient interactions to produce a state that is primed for domain swapping.

■ ASSOCIATED CONTENT

Supporting Information

Figures showing thermal denaturation, NMR spectra of the CytD monomer and dimer with shift analysis, intermolecular NOEs, dihedral angle differences between the monomer and dimer, heteronuclear amide NOEs, van't Hoff plots for dimerization in the absence and presence of Fos16, amide proton protection factors for the monomer and dimer, rate profiles in the presence of detergents or urea, and an Eyring plot for CytD in the presence of Fos16 and a table of structural statistics for the dimer. This material is available free of charge via the Internet at http://pubs.acs.org.

■ AUTHOR INFORMATION

Corresponding Author

*Department of Chemistry, University of Ottawa, 10 Marie Curie, Ottawa, ON K1N 6N5, Canada. E-mail: ngoto@uottawa.ca.

Author Contributions

H.G., J.K.C.K., and A.R.S. contributed equally to this work.

Funding

This work was supported by an NSERC Discovery grant to N.K.G. H.G. was supported by the Sweden-America Foundation and Knut and Alice Wallenberg Foundation, A.C.Y.F. by an Ontario Graduate Scholarship, and J.K.C.K. by an NSERC Postgraduate Scholarship.

Notes

The authors declare no competing financial interest.

■ ACKNOWLEDGMENTS

We are grateful to Jeffrey Keillor for allowing use of his CD spectrometer at the University of Ottawa and to Yves Aubin for acquiring NMR data at the Centre for Vaccine Evaluation, Health Canada, used for assignment of CytD backbone chemical shifts.

■ ABBREVIATIONS

CytD, cytoplasmic domain; DDM, dodecyl maltoside; Fos10, hexadecylphosphocholine; Fos12, dodecylphosphocholine; Fos14, tetradecylphosphocholine; Fos16, hexadecylphosphocholine; LPPG, 1-palmitoyl-2-hydroxy-*sn*-glycero-3-phospho-(1′-*rac*-glycerol); HSQC, heteronuclear single-quantum coherence; CD, circular dichroism.

REFERENCES

(1) Bennett, M. J., Schlunegger, M. P., and Eisenberg, D. (1995) 3D domain swapping: A mechanism for oligomer assembly. *Protein Sci. 4*, 2455−2468.

(2) Gronenborn, A. M. (2009) Protein acrobatics in pairs: Dimerization via domain swapping. *Curr. Opin. Struct. Biol. 19*, 39−49.

(3) Liu, Y., and Eisenberg, D. (2002) 3D domain swapping: As domains continue to swap. *Protein Sci. 11*, 1285−1299.

(4) Huang, Y., Cao, H., and Liu, Z. (2012) Three-dimensional domain swapping in the protein structure space. *Proteins 80*, 1610−1619.

(5) Sue, S.-C., Lee, W.-T., Tien, S.-C., Lee, S.-C., Yu, J.-G., Wu, W.-J., Wu, W.-G., and Huang, T.-H. (2007) PWWP module of human hepatoma-derived growth factor forms a domain-swapped dimer with much higher affinity for heparin. *J. Mol. Biol. 367*, 456−472.

(6) Piccoli, R., Di Donato, A., and D'Alessio, G. (1988) Co-operativity in seminal ribonuclease function. Kinetic studies. *Biochem. J. 253*, 329−336.

(7) Guo, Z., and Eisenberg, D. (2006) Runaway domain swapping in amyloid-like fibrils of T7 endonuclease I. *Proc. Natl. Acad. Sci. U.S.A. 103*, 8042−8047.

(8) Bennett, M. J., Sawaya, M. R., and Eisenberg, D. (2006) Deposition diseases and 3D domain swapping. *Structure 14*, 811−824.

(9) Janowski, R., Kozak, M., Jankowska, E., Grzonka, Z., Grubb, A., Abrahamson, M., and Jaskolski, M. (2001) Human cystatin C, an amyloidogenic protein, dimerizes through three-dimensional domain swapping. *Nat. Struct. Biol. 8*, 316−320.

(10) Liu, C., Sawaya, M. R., and Eisenberg, D. (2011) β_2-Microglobulin forms three-dimensional domain-swapped amyloid fibrils with disulfide linkages. *Nat. Struct. Mol. Biol. 18*, 49−55.

(11) Yamasaki, M., Sendall, T. J., Pearce, M. C., Whisstock, J. C., and Huntington, J. A. (2011) Molecular basis of α1-antitrypsin deficiency revealed by the structure of a domain-swapped trimer. *EMBO Rep. 12*, 1011−1017.

(12) Wahlbom, M., Wang, X., Lindström, V., Carlemalm, E., Jaskolski, M., and Grubb, A. (2007) Fibrillogenic oligomers of human cystatin C are formed by propagated domain swapping. *J. Biol. Chem. 282*, 18318−18326.

(13) Nilsson, M., Wang, X., Rodziewicz-Motowidlo, S., Janowski, R., Lindström, V., Onnerfjord, P., Westermark, G., Grzonka, Z., Jaskolski, M., and Grubb, A. (2004) Prevention of domain swapping inhibits dimerization and amyloid fibril formation of cystatin C: Use of engineered disulfide bridges, antibodies, and carboxymethylpapain to stabilize the monomeric form of cystatin C. *J. Biol. Chem. 279*, 24236−24245.

(14) Sanders, A., Jeremy Craven, C., Higgins, L. D., Giannini, S., Conroy, M. J., Hounslow, A. M., Waltho, J. P., and Staniforth, R. A. (2004) Cystatin forms a tetramer through structural rearrangement of domain-swapped dimers prior to amyloidogenesis. *J. Mol. Biol. 336*, 165−178.

(15) Knaus, K. J., Morillas, M., Swietnicki, W., Malone, M., Surewicz, W. K., and Yee, V. C. (2001) Crystal structure of the human prion protein reveals a mechanism for oligomerization. *Nat. Struct. Biol. 8*, 770−774.

(16) Lee, S., and Eisenberg, D. (2003) Seeded conversion of recombinant prion protein to a disulfide-bonded oligomer by a reduction-oxidation process. *Nat. Struct. Biol. 10*, 725−730.

(17) Chen, Y. W., Stott, K., and Perutz, M. F. (1999) Crystal structure of a dimeric chymotrypsin inhibitor 2 mutant containing an inserted glutamine repeat. *Proc. Natl. Acad. Sci. U.S.A. 96*, 1257−1261.

(18) Barrientos, L. G., Louis, J. M., Botos, I., Mori, T., Han, Z., O'Keefe, B. R., Boyd, M. R., Wlodawer, A., and Gronenborn, A. M. (2002) The domain-swapped dimer of cyanovirin-N is in a metastable folded state: Reconciliation of X-ray and NMR structures. *Structure 10*, 673−686.

(19) Seeliger, M. A., Schymkowitz, J. W. H., Rousseau, F., Wilkinson, H. R., and Itzhaki, L. S. (2002) Folding and association of the human cell cycle regulatory proteins ckshs1 and ckshs2. *Biochemistry 41*, 1202−1210.

(20) Hayes, M. V., Sessions, R. B., Brady, R. L., and Clarke, A. R. (1999) Engineered assembly of intertwined oligomers of an immunoglobulin chain. *J. Mol. Biol. 285*, 1857−1867.

(21) Rousseau, F., Schymkowitz, J. W., Wilkinson, H. R., and Itzhaki, L. S. (2001) Three-dimensional domain swapping in p13suc1 occurs in the unfolded state and is controlled by conserved proline residues. *Proc. Natl. Acad. Sci. U.S.A. 98*, 5596−5601.

(22) Kuhlman, B., O'Neill, J. W., Kim, D. E., Zhang, K. Y., and Baker, D. (2001) Conversion of monomeric protein L to an obligate dimer by computational protein design. *Proc. Natl. Acad. Sci. U.S.A. 98*, 10687−10691.

(23) Rousseau, F., Schymkowitz, J. W. H., Wilkinson, H. R., and Itzhaki, L. S. (2002) The structure of the transition state for folding of domain-swapped dimeric p13suc1. *Structure 10*, 649−657.

(24) Schymkowitz, J. W., Rousseau, F., Irvine, L. R., and Itzhaki, L. S. (2000) The folding pathway of the cell-cycle regulatory protein p13suc1: Clues for the mechanism of domain swapping. *Structure 8*, 89−100.

(25) Jerala, R., and Zerovnik, E. (1999) Accessing the global minimum conformation of stefin A dimer by annealing under partially denaturing conditions. *J. Mol. Biol. 291*, 1079−1089.

(26) Lees, J. P. B., Manlandro, C. M., Picton, L. K., Tan, A. Z. E., Casares, S., Flanagan, J. M., Fleming, K. G., and Hill, R. B. (2012) A designed point mutant in Fis1 disrupts dimerization and mitochondrial fission. *J. Mol. Biol. 423*, 143−158.

(27) Ekeowa, U. I., Freeke, J., Miranda, E., Gooptu, B., Bush, M. F., Pérez, J., Teckman, J., Robinson, C. V., and Lomas, D. A. (2010) Defining the mechanism of polymerization in the serpinopathies. *Proc. Natl. Acad. Sci. U.S.A. 107*, 17146−17151.

(28) Sherratt, A. R., Blais, D. R., Ghasriani, H., Pezacki, J. P., and Goto, N. K. (2012) Activity-based protein profiling of the *Escherichia coli* GlpG rhomboid protein delineates the catalytic core. *Biochemistry 51*, 7794−7803.

(29) Atkins, P., and de Paula, J. (2010) *Atkins' Physical Chemistry*, Oxford University Press, New York.

(30) Delaglio, F. F., Grzesiek, S. S., Vuister, G. W. G., Zhu, G. G., Pfeifer, J. J., and Bax, A. A. (1995) NMRPipe: A multidimensional spectral processing system based on UNIX pipes. *J. Biomol. NMR 6*, 277−293.

(31) Johnson, B. A., and Blevins, R. A. (1994) NMR View: A computer program for the visualization and analysis of NMR data. *J. Biomol. NMR 4*, 603−614.

(32) Cornilescu, G., Delaglio, F., and Bax, A. (1999) Protein backbone angle restraints from searching a database for chemical shift and sequence homology. *J. Biomol. NMR 13*, 289−302.

(33) Güntert, P. (2004) Automated NMR structure calculation with CYANA. *Methods Mol. Biol. 278*, 353−378.

(34) Sreerama, N., and Woody, R. W. (1993) A self-consistent method for the analysis of protein secondary structure from circular dichroism. *Anal. Biochem. 209*, 32−44.

(35) Sreerama, N., and Woody, R. W. (2000) Estimation of protein secondary structure from circular dichroism spectra: Comparison of CONTIN, SELCON, and CDSSTR methods with an expanded reference set. *Anal. Biochem. 287*, 252−260.

(36) Pollard, T. D. (2010) A guide to simple and informative binding assays. *Mol. Biol. Cell 21*, 4061−4067.

(37) Wishart, D. S., and Sykes, B. D. (1994) The ^{13}C chemical-shift index: A simple method for the identification of protein secondary structure using ^{13}C chemical-shift data. *J. Biomol. NMR 4*, 171−180.

(38) Wishart, D. S., Sykes, B. D., and Richards, F. M. (1992) The chemical shift index: A fast and simple method for the assignment of protein secondary structure through NMR spectroscopy. *Biochemistry 31*, 1647−1651.

(39) Lazareno-Saez, C., Arutyunova, E., Coquelle, N., and Lemieux, M. J. (2013) Domain swapping in the cytoplasmic domain of the *Escherichia coli* rhomboid protease. *J. Mol. Biol. 425*, 1127−1142.

(40) Del Rio, A., Dutta, K., Chavez, J., Ubarretxena-Belandia, I., and Ghose, R. (2007) Solution structure and dynamics of the N-terminal cytosolic domain of rhomboid intramembrane protease from

Pseudomonas aeruginosa: Insights into a functional role in intramembrane proteolysis. *J. Mol. Biol. 365*, 109−122.
(41) Sherratt, A. R., Braganza, M. V., Nguyen, E., Ducat, T., and Goto, N. K. (2009) Insights into the effect of detergents on the full-length rhomboid protease from *Pseudomonas aeruginosa* and its cytosolic domain. *Biochim. Biophys. Acta 1788*, 2444−2453.
(42) Dwars, T., Paetzold, E., and Oehme, G. (2005) Reactions in micellar systems. *Angew. Chem., Int. Ed. 44*, 7174−7199.
(43) Magler, I., Nüss, D., Hauser, M., Ferreira, F., and Brandstetter, H. (2010) Molecular metamorphosis in polcalcin allergens by EF-hand rearrangements and domain swapping. *FEBS J. 277*, 2598−2610.
(44) Hsu, Y. T., and Youle, R. J. (1997) Nonionic detergents induce dimerization among members of the Bcl-2 family. *J. Biol. Chem. 272*, 13829−13834.
(45) Czabotar, P. E., Westphal, D., Dewson, G., Ma, S., Hockings, C., Fairlie, W. D., Lee, E. F., Yao, S., Robin, A. Y., Smith, B. J., Huang, D. C. S., Kluck, R. M., Adams, J. M., and Colman, P. M. (2013) Bax crystal structures reveal how BH3 domains activate Bax and nucleate its oligomerization to induce apoptosis. *Cell 152*, 519−531.
(46) Rossmann, M., Schultz-Heienbrok, R., Behlke, J., Remmel, N., Alings, C., Sandhoff, K., Saenger, W., and Maier, T. (2008) Crystal structures of human saposins C and D: Implications for lipid recognition and membrane interactions. *Structure 16*, 809−817.
(47) Hawkins, C. A., de Alba, E., and Tjandra, N. (2005) Solution structure of human saposin C in a detergent environment. *J. Mol. Biol. 346*, 1381−1392.
(48) Liu, L., Byeon, I.-J. L., Bahar, I., and Gronenborn, A. M. (2012) Domain swapping proceeds via complete unfolding: A ^{19}F- and ^{1}H-NMR study of the cyanovirin-N protein. *J. Am. Chem. Soc. 134*, 4229−4235.
(49) Kim, Y. E., Hipp, M. S., Bracher, A., Hayer-Hartl, M., and Hartl, F. U. (2013) Molecular chaperone functions in protein folding and proteostasis. *Annu. Rev. Biochem. 82*, 323−355.
(50) Sharma, S., Chakraborty, K., Mueller, B. K., Astola, N., Tang, Y.-C., Lamb, D. C., Hayer-Hartl, M., and Hartl, F. U. (2008) Monitoring protein conformation along the pathway of chaperonin-assisted folding. *Cell 133*, 142−153.
(51) Lin, Z., Madan, D., and Rye, H. S. (2008) GroEL stimulates protein folding through forced unfolding. *Nat. Struct. Mol. Biol. 15*, 303−311.
(52) Khodarahmi, R., and Yazdanparast, R. (2005) Fluorimetric study of the artificial chaperone-assisted renaturation of carbonic anhydrase: A kinetic analysis. *Int. J. Biol. Macromol. 36*, 191−197.
(53) Morimoto, N., Ogino, N., Narita, T., and Akiyoshi, K. (2009) Enzyme-responsive artificial chaperone system with amphiphilic amylose primer. *J. Biotechnol. 140*, 246−249.
(54) Sampathkumar, P., Mak, M. W., Fischer-Witholt, S. J., Guigard, E., Kay, C. M., and Lemieux, M. J. (2012) Oligomeric state study of prokaryotic rhomboid proteases. *Biochim. Biophys. Acta 1818*, 3090−3097.
(55) Arutyunova, E., Panwar, P., Skiba, P. M., Gale, N., Mak, M. W., and Lemieux, M. J. (2014) Allosteric regulation of rhomboid intramembrane proteolysis. *EMBO J. 33*, 1869−1881.
(56) Schlunegger, M. P., Bennett, M. J., and Eisenberg, D. (1997) Oligomer formation by 3D domain swapping: A model for protein assembly and misassembly. *Adv. Protein Chem. 50*, 61−122.
(57) Bondar, A.-N., Val, C. D., and White, S. H. (2009) Rhomboid protease dynamics and lipid interactions. *Structure 17*, 395−405.
(58) Zhou, Y., Moin, S. M., Urban, S., and Zhang, Y. (2012) An internal water-retention site in the rhomboid intramembrane protease GlpG ensures catalytic efficiency. *Structure 20*, 1255−1263.
(59) Reddy, T., and Rainey, J. K. (2012) Multifaceted substrate capture scheme of a rhomboid protease. *J. Phys. Chem. B 116*, 8942−8954.
(60) Domanska, K., Vanderhaegen, S., Srinivasan, V., Pardon, E., Dupeux, F., Marquez, J. A., Giorgetti, S., Stoppini, M., Wyns, L., Bellotti, V., and Steyaert, J. (2011) Atomic structure of a nanobody-trapped domain-swapped dimer of an amyloidogenic β2-microglobulin variant. *Proc. Natl. Acad. Sci. U.S.A. 108*, 1314−1319.
(61) Sambashivan, S., Liu, Y., Sawaya, M. R., Gingery, M., and Eisenberg, D. (2005) Amyloid-like fibrils of ribonuclease A with three-dimensional domain-swapped and native-like structure. *Nature 437*, 266−269.
(62) Xue, W.-F., Homans, S. W., and Radford, S. E. (2008) Systematic analysis of nucleation-dependent polymerization reveals new insights into the mechanism of amyloid self-assembly. *Proc. Natl. Acad. Sci. U.S.A. 105*, 8926−8931.
(63) Skerget, K., Vilfan, A., Pompe-Novak, M., Turk, V., Waltho, J. P., Turk, D., and Zerovnik, E. (2009) The mechanism of amyloid-fibril formation by stefin B: Temperature and protein concentration dependence of the rates. *Proteins 74*, 425−436.
(64) Serio, T. R., Cashikar, A. G., Kowal, A. S., Sawicki, G. J., Moslehi, J. J., Serpell, L., Arnsdorf, M. F., and Lindquist, S. L. (2000) Nucleated conformational conversion and the replication of conformational information by a prion determinant. *Science 289*, 1317−1321.
(65) Koradi, R., Billeter, M., and Wuthrich, K. (1996) MOLMOL: A program for display and analysis of macromolecular structures. *J. Mol. Graphics 14*, 51−55.